DOI: 10.1002/ejoc.201001196

Comprehensive DFT Study on Site-, Regio-, and Stereoselectivity of Diels–Alder Reactions Leading to 5-Hydroxybenzofurans

Romina Brasca,[a][‡] María N. Kneeteman,[a] Pedro M. E. Mancini,[a] and Walter M. F. Fabian*[b]

Keywords: Cycloaddition / Oxygen heterocycles / Reaction mechanisms / Density functional calculations / Diels–Alder reactions

Diels–Alder reactions between the substituted furans **1a**–**1c** and Danishefsky's diene (**2**), yielding 5-hydroxybenzofurans, were studied by density functional theory [B3LYP/6-31G(d) level] in benzene as solvent (SP/CPCM). The mechanistic details of these reactions, especially with respect to regio-, site-, and stereochemistry were analyzed in detail. Moreover, the extrusion of nitrous acid from the Diels–Alder cycloadducts and the formation of the aromatic products were also explained in order to give a total description of the complete domino processes.

Introduction

Diels–Alder (DA) cycloadditions with furans substituted with electron-withdrawing groups as dienophiles and Danishefsky's diene have been proposed as reliable procedures for the synthesis of benzofuran derivatives.[1] In the three reactions studied, the cycloaddition products showed extrusion of the nitro group, hydrolysis of the silyl enol ether, and elimination of methanol to give the corresponding 5-hydroxybenzofurans (Scheme 1). In principle, eight primary DA adducts – two site-, regio-, and stereoisomers – are possible. The main purpose of this work is to provide a detailed description of these various reaction paths by density functional theory (DFT).

In the last years, new DFT-based concepts and indexes, based on the pioneering work of Parr and Pearson,[2] have been developed to allow modeling of chemical reactivity.[3,4] These conceptual DFT-based descriptors have been successfully applied to interpret reactivity or site-selectivity in different cycloaddition reactions.[5] For the reactions shown in Scheme 1, for instance, we demonstrated that the local electrophilicity (ω_k) and nucleophilicity (N_k) can be used to explain the observed regioselectivity.[6]

More recently we studied the regio- and stereoselectivity of the same series of DA reactions using some global reactivity indexes of the corresponding cycloadducts (i.e., hardness, electrophilicity, and polarizability) and it was confirmed that both the electrophilicities of the adducts and the hardness could be utilized as indicators of regioselectivity and stereoselectivity.[7]

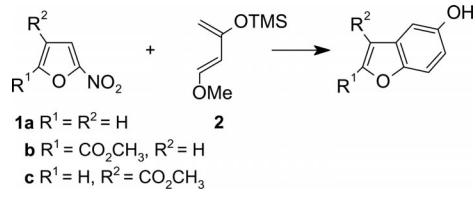

Scheme 1. DA reactions between furan derivatives acting as dienophiles and Danishefsky's diene (diene/dienophile ratio 2:1, benzene, 120 °C, 72 h).[1]

Although the results obtained by use of the local and global indexes were demonstrated to be good for modeling of the reactions studied here, we decided to perform calculations on all eight possible reaction channels (Scheme 2) in order to provide a more detailed description of the transition states and products for study of the site-, regio-, and stereochemistry of these cycloaddition reactions. Therefore, as a complement to the studies previously carried out in our groups and as a contribution to the general knowledge in the field, a complete description of the mechanism of the reactions shown in Scheme 2 was produced.

Results and Discussion

Our main objective was to explain the formation of 5-hydroxybenzofurans from the reaction between the nitrofurans **1a**–**c** and Danishefsky's diene (**2**, Scheme 1).

Firstly, the mechanistic details for the DA reactions between **1a**–**c** and **2** were studied, with special emphasis on

[a] Área de Química Orgánica, Departamento de Química, Facultad de Ingeniería Química, Universidad Nacional del Litoral,
Santiago del Estero 2829, (S3000AOM) Santa Fe, Argentina
[b] Institut für Chemie, Karl-Franzens-Universität Graz,
Heinrichstrasse 28, 8010 Graz, Austria
Fax: +43-316-380-9840
E-mail: walter.fabian@uni-graz.at
[‡] Doctoral scholarship holder from the National Council of Scientific and Technical Research (CONICET)
Supporting information for this article is available on the WWW under http://dx.doi.org/10.1002/ejoc.201001196.

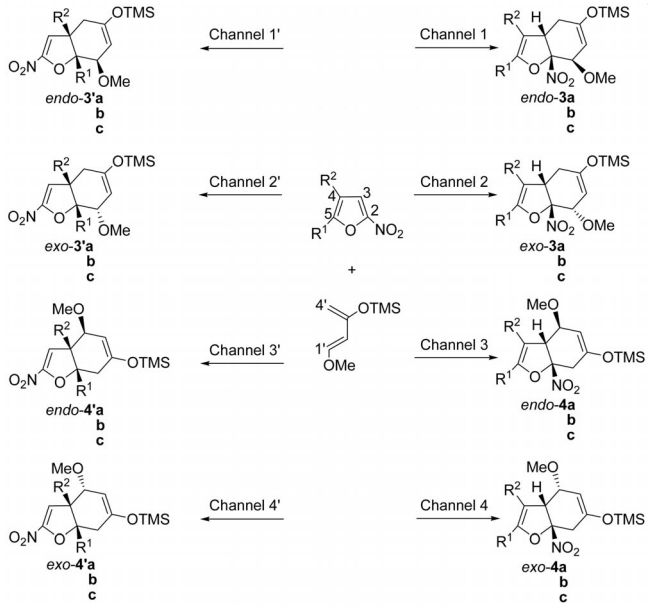

Scheme 2. Possible reaction channels for the cycloadditions between the furan derivatives and Danishefsky's diene.

site-, regio-, and stereoselectivity. Then, the elimination of nitrous acid from the primary cycloadducts was considered. Finally, the tautomeric equilibria between the keto and the aromatic phenol forms of the final products were characterized.

Mechanistic Considerations for the DA Reactions

In the cases considered here, eight channels are feasible for each reaction: two regioisomeric and two stereoisomeric modes of addition for each one of the two endocyclic C=C double bonds of the dienophile, leading both to the *endo* and to the *exo* stereoisomers of the site- and regioisomers **3a**–**c**, **3′a**–**c**, **4a**–**c**, and **4′a**–**c** (Scheme 2). For site isomers resulting from attack of the diene at the nitro-substituted furan double bonds (channels 1–4), *endo*/*exo* stereochemistry is defined by the orientation of the diene subunit with respect to the nitro group. Analogously, for site isomers resulting from reaction of the dienophiles' C4–C5 double bonds (channels 1′–4′), the same *endo*/*exo* notation was maintained. Furthermore, for easier comparison identical atom numbering is used for all three furan derivatives **1a**–**c** (see Scheme 2).

Geometries of the Transition Structures

More than forty TSs were characterized. As an example, the TS corresponding to channel 1 in the reaction between the nitrofuran **1b** and the diene **2** is shown in Figure 1. The forming bonds have substantially different lengths (1.96 and 2.81 Å) and the normal mode corresponding to the imaginary frequency (402i, 397i, and 387i cm^{-1} for the DA reactions involving **1a**, **1b** and **1c**, respectively) indicates bond formation at both ends of the diene in a highly asynchronous motion. All of the cycloadditions therefore show features of a concerted but asynchronous DA process. Pertinent structural parameters are summarized in Table 1 and in Tables S1 and S2 in the Supporting Information. Wiberg and synchronicity indexes of the forming single bonds for the reactions proceeding through channel 1 are shown in Table 2. These calculated bond indexes also show that bonding between C3 of the dienophile and C4′ of the diene in the TS is more advanced than the corresponding bond between C2 and C1′. The estimated synchronicity index is 0.71–0.74, indicating that the processes are slightly asynchronous (25–29%), comparable to the cycloaddition reactions between ketenes and carbonyl compounds.[8] The synchronicity index for formation of the corresponding re-

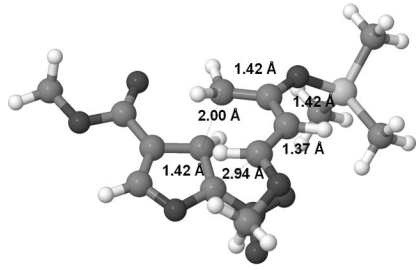

Figure 1. Geometry of the TS structure involved in the minimum-energy reaction pathway for the DA reaction between **1c** and **2** for channel 1.

Table 1. Lengths of the forming $C_{dienophile}$–C_{diene} bonds for all the channels. All values are in Å.[a]

Dienophile	Conformer	Stereoisomer	Channels 1 and 2		Channels 3 and 4		Channels 1′ and 2′		Channels 3′ and 4′	
			C_2–$C_{1'}$	C_3–$C_{4'}$	C_2–$C_{4'}$	C_3–$C_{1'}$	C_5–$C_{1'}$	C_4–$C_{4'}$	C_4–$C_{1'}$	C_5–$C_{4'}$
1a	–	*endo*	2.84	1.96	1.89	2.68	2.01	2.36	3.03	1.85
		exo	2.75	1.91	1.92	2.64	1.93	2.38	3.23	1.89
1b	*s-trans*	*endo*	2.81	1.96	1.88	2.94	2.60	1.94	2.83	1.75
		exo	2.64	1.92	1.87	3.06	2.52	1.91	3.15	1.82
	s-cis	*endo*	2.83	1.96	1.88	2.93	2.66	1.93	2.90	1.81
		exo	2.70	1.91	1.87	3.03	2.54	1.90	3.12	1.84
1c	*s-trans*	*endo*	2.94	2.00	1.86	2.82	1.88	2.51	3.13	1.95
		exo	2.92	1.91	1.93	2.69	1.78	2.56	3.28	2.01
	s-cis	*endo*	2.92	1.99	1.87	2.83	1.89	2.56	3.17	1.98
		exo	2.87	1.91	1.94	2.66	1.77	2.57	3.33	2.02

[a] Both possible orientations of the ester carbonyl group with respect to the endocyclic C=C double bond, *s-cis* and *s-trans*, were taken into consideration.

gioisomer *endo*-**4c** (channel 3) is slightly higher (*Sy* = 0.78). For the analogous site isomer *endo*-**4′c** (channel 3′), for which a two-step mechanism was obtained (see below), *Sy* is only slightly lower (*Sy* = 0.69).

Table 2. Wiberg bond indexes for the newly forming bonds and synchronicity indexes for channel 1.

Dienophile	Conformer	*Sy*	BC_2–$C_{1'}$		BC_3–$C_{4'}$	
			TS	Product	TS	Product
1a	–	0.7368	0.0831	0.9382	0.5342	0.9730
1b	*s-trans*	0.7459	0.0868	0.9374	0.5377	0.9710
	s-cis	0.7405	0.0846	0.9378	0.5384	0.9707
1c	*s-trans*	0.7114	0.0643	0.9379	0.5035	0.9725
	s-cis	0.7172	0.0668	0.9383	0.5099	0.9729
1c[a]	*s-trans*	0.7751	0.5887	0.9866	0.1546	0.9581

[a] Channel 3.

Generally, distances to C1′ of the diene are substantially longer (2.4–3.3 Å) than those to C4′ (1.7–2.0 Å). As a consequence, C4′ of the diene and the corresponding carbon atom of the dienophile (e.g., C3 in channels 1 and 2) are significantly pyramidalized, as evidenced by the sums of the angles around these atoms ($\Sigma\alpha$ = 340–350°). In contrast, no pyramidalization is indicated for the two other carbon atoms: C1′ of the diene and, in the cases of channels 1 and 2, C2 of the dienophile ($\Sigma\alpha \approx 360°$). The more advanced formation of bonding to C4′ of the diene is also reflected in the changes of other relevant bond lengths in the diene subunit: an increase in *r*(C3′–C4′) from 1.35 to 1.43–1.46 Å, a decrease in *r*(C2′–C3′) from 1.47 to 1.40–1.44 Å, and a much smaller elongation of *r*(C1′–C2′) than found for *r*(C3′–C4′), from 1.34 to 1.36–1.39 Å. These geometric changes are accompanied by corresponding changes in the electronic structures, as revealed by NBO analysis. In the TS for the reaction **1c** + **2** according to channel 1, for instance, a nearly doubly occupied bonding orbital between C3 and C4′ has already evolved (occupancy: 1.78) at the expense of the C2–C3 and C3′–C4′ π bonds. The "partner" p_z-AOs of these broken π bonds are transformed into lone pairs mainly localized at C2 (occupancy: 1.18) and C3′ (occupancy: 0.88), respectively. In contrast with C3′–C4′, the C1′–C2′ π bond is still largely intact (occupancy: 1.78) with some delocalization involving the lone pair at C3′. The lone pair at C2 is stabilized by delocalization into the nitro group. Relevant NBOs of the channel 1 TS for the reaction **1c** + **2** are depicted in Figure S1 in the Supporting Information.

The only exceptions to these quite general structural changes on going to the transition states are the reactions of **1a** and **1c** according to channels 1′ and 2′: formation of the bond to C1′ of the diene here is significantly more advanced than that to C4′, with other concomitant structural changes, such as greater pyramidalization at C1′ than at C4′ (e.g., $\Sigma\alpha$ = 346 and 358°), respectively, for the reaction with **1c** as dienophile, as well as more pronounced elongation of *r*(C1′–C2′) than *r*(C3′–C4′) (Table S2 in the Supporting Information). Only in these reactions does C1′ of the diene interact with the unsubstituted carbon atom C5 of the furan.

Possible explanations for the preferred formation of the bond to C4′ of the diene are: 1) strong interaction between the reactant active sites due to a greater overlap of the orbitals [i.e., the interaction between the most electrophilic site of the dienophile (C3) and the most nucleophilic site of the diene[6] (C4′, see below, Table 3) leads to a stronger bonding], and 2) increased steric interactions between the oxygen substituent at C1′ of the diene and the dienophile's reaction center (C2 for channels 1 and 2). On the other hand, the substituent at the 3-position of the diene lies too far away from the reaction center and does not interfere with the approaching furan sterically in a significant way in any of the TSs. The steric effect exerted by substituents on the reaction center has been analyzed in detailed by Boulanger et al. for a great variety of 1- and 2-substituted buta-1,3-dienes participating in Diels–Alder reactions with ethylene.[9] Only small steric effects were found for 2-substituted dienes, even for barriers related to *endo*/*exo* stereoselectivity. In contrast, steric effects were found to be important for 1-substituted dienes.

Table 3. DFT-based descriptors[a] for the reactive sites of the reactants.[6]

Dienophile	ω_k			Diene	N_k
	1a	**1b**	**1c**		
C_2	0.07 (0.09)	0.16 (0.18)	0.09 (0.11)	$C_{4'}$	1.33 (1.28)
C_3	0.39 (0.42)	0.32 (0.35)	0.43 (0.46)	$C_{1'}$	0.51 (0.50)
C_4	0.01 (0.01)	0.04 (0.04)	0.01 (0.01)		
C_5	0.28 (0.31)	0.33 (0.36)	0.28 (0.30)		

[a] B3LYP/6-31G(d); B3LYP/6-311G(d,p) values in parentheses.

Channels 3′ and 4′ deserve special attention: in several cases for these two channels – **1c** + **2** and the *exo* addition mode for **1a** + **2** – two-step mechanisms involving true intermediates were obtained by the calculations (Figure 2). In contrast, the **1b** + **2** cycloaddition in these two channels should also proceed through a concerted mechanism. Polar cycloadditions between electron-rich and electron-poor π systems are characterized by nucleophilic attack of the electron-rich reactant with concomitant ring closure.[10] Consequently, one might consider these reactions as being initialized by a two-center interaction involving the most electrophilic and nucleophilic sites, respectively, of the two reactants. From conceptual density functional theory, local electrophilicity (ω_k) and nucleophilicity (N_k) have been found to be useful descriptors[11,12] for the quantification of these concepts (Table 3).[6] These descriptors had shown some basis set dependence, so we have recalculated them using the 6-311G(d,p) basis set (values in parentheses in Table 3). No significant changes at all were obtained.

The greatest nucleophilicity of the diene is at C4′, so preferential bond formation to this atom would be anticipated. Except for a longer C4–C1′ distance than found for concerted additions (Table 1), no significant differences exist between the TSs for the concerted and stepwise reaction paths. Likewise, the electronic structures are entirely similar, as revealed by NBO analysis. In the TS for the reaction **1c** + **2** according to channel 4′, for instance, a nearly doubly occupied bonding orbital between C5 and C4′ has already

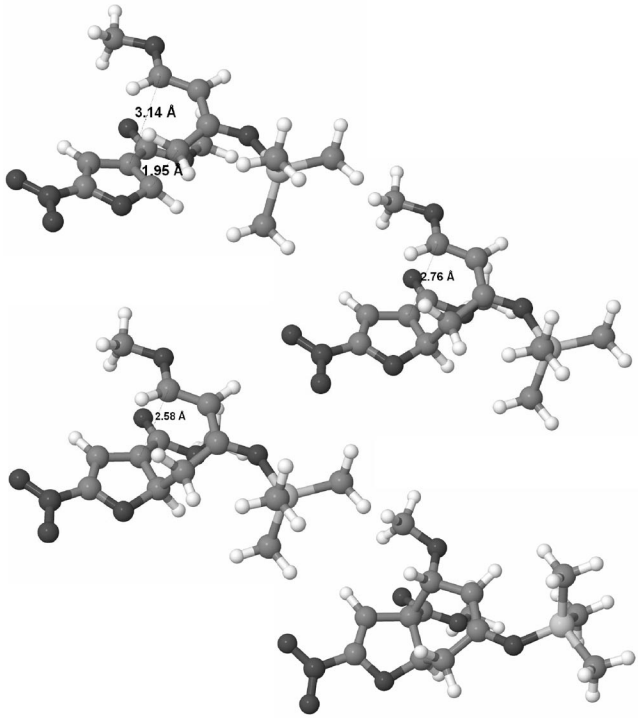

Figure 2. Geometries of the TS structures (TS1: left at top; TS2: left at bottom), the intermediate (right at top), and the product (right at bottom) involved in the DA reaction between **1c** and **2** for channel 3′.

formed (occupancy: 1.71) at the expense of the C4–C5 and C3′–C4′ π bonds. The "partner" p_z-AOs of these broken π bonds are transformed into lone pairs mainly localized at C4 (occupancy: 1.17) and C3′ (occupancy: 0.89), respectively. In contrast with C3′–C4′, the C1′–C2′ π bond is still largely intact (occupancy: 1.81), with some delocalization involving the lone pair at C3′. The lone pair at C4 is stabilized by delocalization into the ester carbonyl group. The newly formed C5–C4′ bond is somewhat weakened by occupation of the corresponding antibonding orbital (occupancy: 0.34). A similar weakening is also seen for the analogous C3–C4′ bond formed in the reaction along channel 1 (occupancy: 0.30). Relevant NBOs of the first TS in channel 4′ for the reaction **1c** + **2** are depicted in Figure S1 in the Supporting Information. Independently of the substitution patterns of the dienophiles **1a**–**c**, the highest values of local electrophilicity are at C3 and, to a lesser extent, C5. Consequently, on the basis of conceptual density functional theory, channels 1 and 2 would be predicted to be the preferred reaction paths,[6] although attack at C5 cannot be completely ruled out. Moreover, ω_k values are particularly low at C4 of the dienophile, especially for **1a** and **1c**. Interaction of these centers with the diene would be very weak, possibly resulting in two-step reactions for channels 3′ and 4′. From the above discussion it is evident that quite subtle structural changes can be decisive for whether these cycloadditions proceed in concerted or stepwise fashion with little difference in the geometric and electronic structures of the corresponding transition states.

Energetics of the DA Reactions

Calculated activation and reaction energies (ΔE_{act} and ΔE_{react}) including ZPE corrections in benzene as solvent for all site-, regio-, and stereoisomeric reaction paths are summarized in Table 4. The corresponding gas-phase data are provided in Table S3 in the Supporting Information. Generally, the effect of the solvent benzene as determined by CPCM single-point calculations leads to preferential stabilization of the reactants with concomitant increases and decreases in ΔE_{act} and ΔE_{react}, respectively.

With regard to stereochemistry, the *endo* stereoisomers are usually formed preferentially, except in the cases of cycloadducts resulting from reactions of **1a** and **1c** according to channels 3′ and 4′. The activation energies are slightly lower than for *exo* addition and the resulting products are more stable. The highest barriers are calculated for cycloadditions involving bond formation between C5–C1′ and C4–C4′ (channels 1′ and 2′), so reactions along these two paths can safely be ruled out. Similarly, except for **1b**, in which quite small differences are found (Table 4), the ΔE_{act} values for channels 3 and 4 are significantly higher than for channels 1 and 2. Channels 3′ and 4′ require special attention: as pointed out above, these two channels are prone to stepwise rather than concerted reaction mechanisms. Similar stepwise mechanisms with polar characters and low activation energies have already been found for DA reactions involving electron-rich dienes (nucleophiles) and electron-deficient dienophiles (electrophiles), such as nitronaphthalenes.[13] Many cycloadditions proceeding through stepwise mechanisms have lower activation energies than concerted ones.[4,10,14] In fact, some researchers have demonstrated that the more asynchronous the TS, the lower the barriers.[15] Here we find rather low activation energies for channels 3′ and especially 4′ (*exo* addition) except in the case of the reaction of **1b**, which follows a concerted mechanism. However, the resulting products are generally considerably less stable than those formed in channels 1 or 2. From the B3LYP/6-31G(d)-calculated activation energies, formation of *endo*-**3b**, *exo*-**4′a**, and *exo*-**4′c** would be expected.

M06-2X/cc-pVTZ calculations for the reaction of *s-trans* **1c** + **2**, combined with SM8-M06-2X/6-31+G(d,p) solvation energies (benzene solution), generally result in lower activation energies, especially for concerted reactions, and greater exothermicities (Table 4). However, the overall picture does not change. Similarly, on consideration of Gibbs free energies of activation and reaction, ΔG_{act} and ΔG_{react} (see Table S4 in the Supporting Information) do not change the conclusions based on ZPE-corrected energies in a qualitative sense. However, quantitatively significant differences result. Most importantly, besides increases in the reaction barriers, all cycloadditions resulting from channels 1′–4′ (i.e., addition to the C4–C5 double bonds in **1a**–**1c**), are endergonic with the single exception of the *endo* addition to **1a**. Gibbs free energies of activation for formation of cycloadducts according to channels 3′ and 4′ are still lower than those proceeding along channel 1. However, formation of the corresponding products is endergonic. Consequently,

Table 4. Relative energies (kcal mol^{-1}) of the stationary points involved in the DA reactions with Danishefsky's diene for all eight channels in benzene as solvent.[a]

Dienophile	Conformer	Stereoisomer	Channels 1 and 2		Channels 3 and 4		Channels 1′ and 2′		Channels 3′ and 4′	
			ΔE_{act}	ΔE_{react}	ΔE_{act}	ΔE_{react}	ΔE_{act}	ΔE_{react}	ΔE_{act}	ΔE_{react}
1a	–	*endo*	19.6	–15.0	25.6	–15.7	30.6	–12.7	18.5	–12.9
		exo	21.2	–12.9	26.8	–15.5	30.5	–9.1	17.1[b]	–12.7
									15.7[c]	
									15.8[d]	
1b	*s-trans*	*endo*	18.9	–15.1	19.1	–16.0	25.9	–8.2	21.5	–8.8
		exo	20.7	–11.1	19.4	–16.0	27.6	–5.7	19.3	–8.5
	s-cis	*endo*	18.9	–15.0	19.4	–15.9	25.4	–8.0	21.7	–6.6
		exo	20.7	–13.1	19.9	–15.8	26.6	–6.0	19.2	–8.5
1c	*s-trans*	*endo*	16.1	–18.5	22.3	–19.0	27.9	–7.6	12.3 (10.9)[b]	–6.2
			(14.6)	(–29.3)	(19.8)	(–29.4)	(25.0)	(–17.8)	9.4 (7.6)[c]	(–17.7)
									10.0 (7.5)[d]	
		exo	16.5	–16.4	23.3	–17.5	27.9	–4.6	10.0 (9.7)[b]	–7.4
			(14.6)	(–28.1)	(20.0)	(–28.8)	(23.8)	(–15.6)	5.6 (5.6)[c]	(–18.1)
									8.5 (7.1)[d]	
	s-cis	*endo*	16.4	–18.2	23.1	–16.4	27.4	–8.3	12.8[b]	–7.0
									9.2[c]	
									17.2[d]	
		exo	17.5	–16.2	24.0	–16.8	28.0	–3.1	9.8[b]	–7.1
									5.1[c]	
									7.7[d]	

[a] Activation energies (ΔE_{act}) and reaction energies (ΔE_{react}), obtained from CPCM (solvent: benzene) single-point calculations on gas-phase geometries, are given relative to the separated reactants. ZPE corrections are included. Values for the reaction of *s-trans* **1c** in parentheses are from M06-2X/cc-pVTZ//B3LYP/6-31G(d) single-point calculations with SM8-M06-2X/6-31+G(d,p) solvation energies. [b] TS1. [c] Intermediate. [d] TS2.

reactions leading to cycloadducts **4′a**–**c** will either hardly occur or will lead at best to metastable products (see below).

Experimentally, in all three reactions between Danishefsky's diene (**2**) and the nitrofurans **1a**–**c**, the 5-hydroxybenzofurans **7** (Scheme 1) were obtained.[1] Formation of these products can only be explained by initial formation of cycloadducts according to reaction channel 1. However, it must be stressed that none of these primary cycloadducts could ever be observed. Instead, they underwent subsequent extrusion of nitrous acid (Scheme 3), followed by hydrolysis of the silyl enol ether and elimination of methanol (Scheme 4, below and Scheme 5, below). Consequently, we now turn to a description of the elimination of nitrous acid from the cycloadducts *endo*-**3a**–**c**, formed in the cycloaddition path 1 (Scheme 2). No such extrusion of HNO_2 from site isomers obtained in reaction paths 1′–4′ is possible.

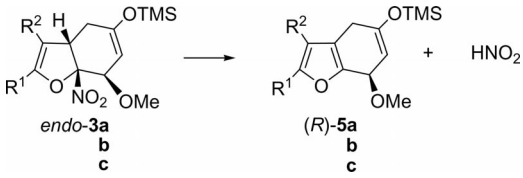

Scheme 3. Extrusion of nitrous acid from the *endo*/nitro DA cycloadducts (channel 1).

Extrusion of Nitrous Acid

Extrusion of nitrous acid is feasible only from cycloadducts formed through reactions according to channels 1–4 (i.e., site isomers resulting from attack of the diene at the nitro-substituted double bond of the furan, Scheme 2). Calculated activation energies for these site isomers are lowest for reactions according to channel 1. The following discussion is thus restricted to elimination of nitrous acid from cycloadducts formed through channel 1: *endo*-**3a**–**c** (Scheme 2). In all cases, concerted *cis* elimination of the nitro group at C9 and the hydrogen atom at C8 was calculated. Relevant structural parameters for the corresponding transition states, as well as activation and reaction energies (ΔE_{act} and ΔE_{react}) with respect to the primary cycloadducts *endo*-**3a**–**c**, are summarized in Table 5. Obviously, in the transition structures the C9–N bond is considerably more elongated than the C8–H bond.

Table 5. Calculated activation and reaction energies (ΔE_{act} and ΔE_{react}, kcal mol^{-1}) for the elimination of nitrous acid from the cycloadducts *endo*-**3a**–**c** and lengths of the forming and breaking bonds (Å). The values obtained in benzene are shown in parentheses.

Reactant	Conformer	C_9–N	C_8–H	O–H	ΔE_{act}	ΔE_{react}
endo-**3a**	–	2.35	1.25	1.41	27.1 (25.9)	–5.5 (–8.0)
endo-**3b**	*s-trans*	2.29	1.26	1.40	26.0 (25.6)	–8.6 (–11.1)
	s-cis				26.1 (25.4)	–8.4 (–11.2)
endo-**3c**	*s-trans*	2.31	1.26	1.39	29.2 (28.7)	–4.7 (–7.0)
	s-cis				29.2 (28.7)	–4.5 (–6.9)

According to the NBO analysis of the TSs, the bond to the nitro group (C9–N in Figure 3) is already broken while the C8–H bond is still largely intact (occupancy of the σ-bond: 1.71, for the antibonding σ*-bond: 0.17). The broken C9–N bond is transformed into a sp-type lone pair at nitrogen (occupancy: 1.79) and a π-bond between C9 and the furan oxygen atom but mainly localized at C9 (occupancy:

1.91, with 0.64 for the corresponding antibonding π*-orbital). The π-type lone pair at the oxygen atom of the NO_2 group pointing towards the hydrogen atom shows some interaction with the NBOs describing the C8–H bond. Relevant NBOs are presented in Figure S2 in the Supporting Information.

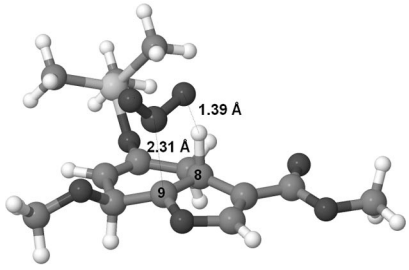

Figure 3. Geometry of the transition structure involved in the minimum-energy reaction pathway for the elimination reaction starting from the cycloadduct *endo*-**3c** (channel 1).

In contrast to the cycloaddition reactions, solvent effects preferentially stabilize the TSs and products of the eliminations. Activation energies in benzene are therefore lowered in relation to the gas phase and reaction exothermicities are increased (Table 5). The barriers for HNO_2 extrusion from the cycloadducts are quite high. However, if the rather large exothermicities of formation of *endo*-**3a**–**c** [ΔE_{react} = –15 (*endo*-**3a**, *endo*-**3b**) and –18.5 kcal mol^{-1} (*endo*-**3c**)] are taken into account, the elimination TSs are still below those for cycloaddition. The complete energetics for cycloaddition according to channel 1 followed by extrusion of HNO_2, as well as for cycloaddition according to channel 4′, are displayed in Figure 4.

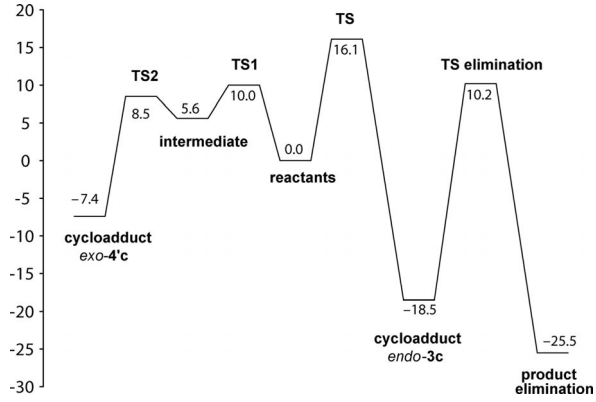

Figure 4. Comparison of the energetic profiles (kcal mol^{-1}) between channel 4′ (left side of the chart) and channel 1 + elimination (right) for **1c**.

Thus, even should some of the DA reactions between the nitrofurans **1a**–**c** and Danishefsky's diene (**2**) preferentially proceed through channels 3′ or 4′ in a kinetically controlled manner (Table 4), under the experimental conditions[1] used [i.e., heating in benzene (ampoule) at 120 °C for 3 days], the subsequent elimination reactions should push the reactions towards the formation of **5a**–**c**. The endergonic natures of the cycloadducts **4′a**–**c** should additionally facilitate reactions according to channels 1 and 2. Although the Gibbs free energies of activation for elimination are only slightly larger than the corresponding ΔE_{act} values, ΔG_{react} are much more negative than ΔE_{react} (Table S5 in the Supporting Information), resulting in additional stabilization of **5a**–**c** with respect to the primary cycloadducts **3a**–**c**. The irreversibility of the elimination step is thus even more pronounced. A Gibbs free energy profile comparison between channel 4′ and channel 1 for **1c**, together with elimination, is shown in Figure S3 in the Supporting Information.

Furthermore, compounds **5a**–**c** are unstable and prone to undergoing further elimination reactions. This susceptibility of several DA cycloadducts, particularly those obtained through reactions with Danishefsky's diene, to various hydrolytic eliminations has been pointed out in many publications.[16–18] The elimination of the methoxy group as methanol concurrently with the hydrolytic conversion of the silyl enol ether to the ketone has in fact been demonstrated for such thermal DA reactions (Scheme 4).[17]

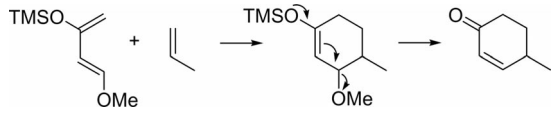

Scheme 4. Hydrolysis of the silyl enol ether and elimination of methanol.

In general, hydrolysis leading to α,β-unsaturated ketones can be done under extremely mild conditions. Hydrolysis of many DA adducts has been observed during purification by classic column chromatography, for instance.[19] In addition, for other types of adducts obtained with 2-siloxy-substituted dienes, the hydrolysis of the silyl enol ethers can be done under essentially neutral conditions through nucleophilic cleavage of the O–Si bond.[20] In certain other DA reactions, spontaneous aromatization can take place in the cyclic ketones, involving the loss of the substituents originally in the 1-positions in the dienes and occasionally the extrusion of the substituent(s) in strategic positions of the dienophiles.[16a,16b,19a,21]

The conversion of the silyl enol ethers **5a**–**c** into the α,β-unsaturated ketones with the elimination of methanol and final aromatization to **7a**–**c** (Scheme 5) can therefore be expected and provides an additional driving force for reaction along channel 1 (or 2).

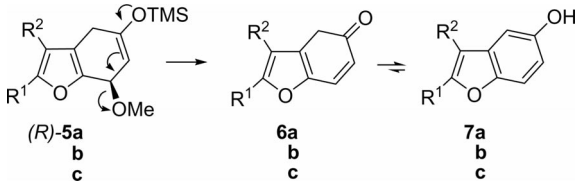

Scheme 5. Hydrolysis of TMS and elimination of MeOH in **5a**, **5b**, and **5c** to afford the aromatic products **7a**, **7b**, and **7c**.

The calculated tautomerization constants for **7a**–**c** in benzene are in the 3.4×10^6 to 1.3×10^7 range. The experimentally measured K_T values for the tautomeric equilibrium phenol ⇆ cyclohexa-2,4-dienone are 5.4×10^{12} in aqueous solution[22] and 1.4×10^{13} in the gas phase.[23] As

expected for proton transfers involving four-membered transition states, activation energies for conversion of the keto to the phenol forms are quite high: $\Delta G_{act} \approx 54$ kcal mol^{-1}, comparable to that obtained for phenol (ΔE_{act} = 53.3 kcal mol^{-1}) by high-level ab initio calculations [CASPT2(8,8)/cc-pVTZ].[24]

Conclusions

The site-, regio-, and stereochemistry of DA reactions between the nitrofurans **1a**–**c** and Danishefsky's diene (**2**) has been investigated by density functional theory [B3LYP/6-31G(d)], including solvent effects (benzene), by CPCM single-point calculations. Generally, these cycloadditions proceed by a concerted but asynchronous reaction mechanism. Only for channel 3′ and, especially, channel 4′ [i.e., isomers resulting from interaction between C5(furan)···C4′(diene) and C4(furan)···C1′(diene)] were stepwise mechanisms found for reactions of the dienophiles **1a** and **1c**. The electronic structures of the various transition states show almost no differences, indicating quite subtle effects leading to concerted or stepwise reactions. Previous conceptual DFT analysis predicted that channels 1 and 2 should be preferred on the basis of the local electrophilicity (ω_k) on C3.[6] However, quite substantial or even equal (**1b**) electrophilicities are obtained for C5 (Table 3). Other factors might thus become important for the regio- or site selectivity of the cycloaddition steps. For instance, electrostatic repulsion between the negative NO_2 group of the dienophile and the methoxy moiety of the diene will likely increase the activation energies for channels 1 and 2. The *endo* stereochemistry is in most cases preferred. The lowest activation energies for concerted reactions are obtained for channel 1. Stepwise additions have significantly lower activation energies but lead to substantially less stable products. Moreover, the primary cycloadducts could never be isolated but were converted into 5-hydroxybenzofurans by subsequent extrusion of nitrous acid, hydrolysis of the silyl enol ether, and elimination of methanol. Elimination of nitrous acid is calculated to have lower overall barriers than cycloaddition reactions and is strongly exothermic, thus explaining the preferred reaction according to channel 1. Barriers for regioisomeric addition to the nitro-substituted double bond of the dienophile (channels 3 and 4) and site isomers resulting from addition to the C4=C5 double bond (channels 1′ and 2′) are generally higher than those for addition according to channels 1 or 2. NBO analysis indicates significant evolution of one of the two newly forming bonds in all transition states, including those of stepwise additions, and essentially no bonding between the second set of reaction centers.

Computational Details

The gas-phase equilibrium geometries of all species described here were obtained by full optimization at the B3LYP/6-31G(d)[25] level. This level of theory was selected because it has been shown to be suitable for modeling of DA reactions involving medium-sized molecules[26] and also allows calculations such as those performed here to be done in a reasonable time. In addition, for selected structures single-point calculations were preformed with use of the M06-2X functional[27] and the cc-pVTZ basis set.[28] Programs used for these calculations were GAUSSIAN 03[29] and NWChem.[30]

1-Methoxy-3-trimethylsiloxybuta-1,3-diene exists in two minimum-energy conformations, the more stable being the *s-trans* arrangement {θ = 180°, ΔE = –2.60 kcal mol^{-1} [B3LYP/6-31G(d)]}.[6] Because the *s-gauche* conformer (θ = 33°) presents the most favorable geometry for cycloaddition, the reaction occurs from this conformer.[31] The diene was therefore considered in the *s-gauche* conformation.

All stationary points were characterized as true minima or transition states by frequency calculations. Transition states were further characterized by intrinsic reaction coordinate (IRC) calculations[32] (15 points along both directions of the normal mode corresponding to the imaginary frequency).

All B3LYP/6-31G(d) calculated energies were corrected for zero-point vibrational effects (ZPE) and the free energy changes for the tautomerization reactions were derived from the sums of the electronic and thermal Gibbs free energies. Zero-point energies and thermal corrections are unscaled.

The synchronicity index of the cycloaddition leading to the observed product (*Sy*) was estimated by use of the Wiberg bond indexes by the following equation[8,33]

$$Sy = 1 - \frac{1}{(2n-2)} \sum_{i=1}^{i=n} \left| \frac{\delta B_i - \delta B_{av}}{\delta B_{av}} \right|$$

where n is the number of bonds directly involved in the cycloaddition reaction

δB_{av} is the average value of δB_i

δB_i is the relative variation of the bond index at the transition state for every bond involved in the reaction and is calculated by the following equation

$$\delta B_i = \frac{B_i^{TS} - B_i^{R}}{B_i^{P} - B_i^{R}}$$

where the superscripts TS, R, and P correspond to the transition state, reactant, and product, respectively.

Solvent effects (benzene solution as used in the experiments[1]) were considered by single-point calculations on the optimized gas-phase structures by use of a polarizable continuum method[34] in its conductor-like approximation (CPCM).[35] Only the electrostatic component of the solvation energy was taken into account. It is important to stress that we found insignificant differences when comparing the structures obtained by this approach with the available solvent-optimized structures, thus providing credence for the single-point calculations. Moreover, it was demonstrated that the inclusion of the solvent during the geometry optimizations did not substantially modify the gas-phase geometries involved in some cycloaddition reactions.[36] For selected structures the SM8[37] solvation model [SM8-M06-2X/6-31+G(d,p)] as implemented in GAMESSPLUS[38] was used to estimate the influence of benzene as a solvent. NBO analysis[39] was performed with the program NBO[40] as implemented in GAUSSIAN 03. Structure manipulation and visualization was done with MOLDEN[41] and Jmol.[42]

Supporting Information (see also the footnote on the first page of this article): Tables for pertinent structural parameters, relative gas phase energies, Gibbs free energies in solution, plots of representa-

tive NBOs, and Gibbs free energy profile for channel 4′ and channel 1 + elimination for **1c**.

Acknowledgments

R. Brasca thanks the Austrian Exchange Service (ÖAD) and the Austrian Federal Ministry of Science and Research (BMWF) for the Ernst-Mach Stipendien, the European Commission for the Erasmus Mundus External Cooperation Window (EMECW) Lot 16 Scholarship, and the Argentine Consejo Nacional de Investigaciones Científicas y Técnicas (CONICET) for a doctoral grant programme.

[1] C. Della Rosa, M. N. Kneeteman, P. M. E. Mancini, *Tetrahedron Lett.* **2005**, *46*, 8711–8714.
[2] R. G. Parr, R. G. Pearson, *J. Am. Chem. Soc.* **1983**, *105*, 7512–7516.
[3] For reviews on conceptual density functional theory, see: a) D. H. Ess, G. O. Jones, K. N. Houk, *Adv. Synth. Catal.* **2006**, *348*, 2337–2361; b) P. Geerlings, F. De Proft, W. Langenaeker, *Chem. Rev.* **2003**, *103*, 1793–1873.
[4] G. Gayatri, G. Narahari Sastry, *J. Chem. Sci.* **2005**, *117*, 573–582.
[5] a) L. R. Domingo, P. Pérez, R. Contreras, *Eur. J. Org. Chem.* **2006**, 498–506; b) S. Noorizadeh, H. Maihami, *THEOCHEM* **2006**, *763*, 133–144; c) L. R. Domingo, P. Pérez, R. Contreras, *Lett. Org. Chem.* **2005**, *2*, 68–78.
[6] R. Brasca, M. N. Kneeteman, P. M. E. Mancini, W. M. F. Fabian, *THEOCHEM* **2009**, *911*, 124–131.
[7] R. Brasca, M. N. Kneeteman, P. M. E. Mancini, W. M. F. Fabian, 13thInternational Electronic Conference on Synthetic Organic Chemistry (ECSOC-13), **2009**.
[8] B. Lecea, A. Arrieta, G. Roa, J. M. Ugalde, F. P. Cossio, *J. Am. Chem. Soc.* **1994**, *116*, 9613–9619.
[9] M. L. Boulanger, T. Leyssens, R. Robiette, D. Peeters, *THEOCHEM* **2005**, *731*, 101–106.
[10] L. R. Domingo, M. Arnó, J. Andrés, *J. Org. Chem.* **1999**, *64*, 5867–5875.
[11] a) E. Chamorro, P. K. Chattaraj, P. Fuentealba, *J. Phys. Chem. A* **2003**, *107*, 7068–7072; b) P. Pérez, A. Toro-Labbé, A. Aizman, R. Contreras, *J. Org. Chem.* **2002**, *67*, 4747–4752; c) L. R. Domingo, M. J. Aurell, P. Pérez, R. Contreras, *J. Phys. Chem. A* **2002**, *106*, 6871–6875.
[12] a) P. Pérez, L. R. Domingo, M. Duque-Noreña, E. Chamorro, *THEOCHEM* **2009**, *895*, 86–91; b) R. Contreras, J. Andrés, V. S. Safont, P. Campodonico, J. G. Santos, *J. Phys. Chem. A* **2003**, *107*, 5588–5593.
[13] L. R. Domingo, M. J. Aurell, M. N. Kneeteman, P. M. E. Mancini, *THEOCHEM* **2008**, *853*, 68–76.
[14] a) L. Legnani, C. Lunghi, F. M. Albini, C. Nativi, B. Richichi, L. Toma, *Eur. J. Org. Chem.* **2007**, 3547–3554; b) H. Wang, Y. Wang, K.-L. Han, X.-J. Peng, *J. Org. Chem.* **2005**, *70*, 4910–4917.
[15] a) M. D. Refvik, R. D. J. Froese, J. D. Goddard, H. H. Pham, M. F. Pippert, A. L. Schwan, *J. Am. Chem. Soc.* **1995**, *117*, 184–192; b) W. L. Jorgensen, D. Lim, J. F. Blake, *J. Am. Chem. Soc.* **1993**, *115*, 2936–2942.
[16] a) C. Della Rosa, M. N. Kneeteman, P. M. E. Mancini, *Tetrahedron Lett.* **2007**, *48*, 7075–7078; b) E. Paredes, R. Brasca, M. N. Kneeteman, P. M. E. Mancini, *Tetrahedron* **2007**, *63*, 3790–3799; c) H. M. I. Osborn, D. Coisson, *Mini-Rev. Org. Chem.* **2004**, *1*, 41–45; d) E. Paredes, B. Biolatto, M. N. Kneeteman, P. M. E. Mancini, *Tetrahedron Lett.* **2002**, *43*, 4601–4603.
[17] a) S. Danishefsky, T. Kitahara, C. F. Yan, J. Morris, *J. Am. Chem. Soc.* **1979**, *101*, 6996–7000; b) S. Danishefsky, T. Kitahara, *J. Am. Chem. Soc.* **1974**, *96*, 7807–7808.
[18] C. D. Donner, M. Gill, L. M. Tewierik, *Molecules* **2004**, *9*, 498–512.
[19] a) E. M. Beccalli, F. Clerici, M. L. Gelmi, *Tetrahedron* **2003**, *59*, 4615–4622; b) S. Danishefsky, M. P. Prisbylla, S. Hiner, *J. Am. Chem. Soc.* **1978**, *100*, 2918–2920.
[20] M. E. Jung, C. A. McCombs, *Tetrahedron Lett.* **1976**, *17*, 2935–2938.
[21] S. Danishefsky, C.-F. Yan, R. K. Singh, R. B. Gammill, P. M. McCurry Jr, N. Fritsch, J. Clardy, *J. Am. Chem. Soc.* **1979**, *101*, 7001–7008.
[22] M. Capponi, I. G. Gut, B. Hellrung, G. Persy, J. Wirz, *Can. J. Chem.* **1999**, *77*, 605–613.
[23] L. Zhu, J. W. Bozzelli, *J. Phys. Chem. A* **2003**, *107*, 3696–3703.
[24] I. Gómez, E. Rodríguez, M. Reguero, *THEOCHEM* **2006**, *767*, 11–18.
[25] a) A. D. Becke, *J. Chem. Phys.* **1993**, *98*, 5648–5652; b) C. Lee, W. Yang, R. G. Parr, *Phys. Rev. B* **1988**, *37*, 785–789.
[26] a) J. Soto-Delgado, L. R. Domingo, R. Araya-Maturana, R. Contreras, *J. Phys. Org. Chem.* **2009**, *22*, 578–584; b) C. N. Alves, A. S. Carneiro, J. Andres, L. R. Domingo, *Tetrahedron* **2006**, *62*, 5502–5509; c) P. Arroyo, M. T. Picher, L. R. Domingo, F. Terrier, *Tetrahedron* **2005**, *61*, 7359–7365; d) K. Geetha, T. C. Dinadayalane, G. N. Sastry, *J. Phys. Org. Chem.* **2003**, *16*, 298–305; e) R. Vijaya, T. C. Dinadayalane, G. N. Sastry, *THEOCHEM* **2002**, *589*, 291–299; f) L. R. Domingo, M. T. Picher, M. J. Aurell, *J. Phys. Chem. A* **1999**, *103*, 11425–11430; g) L. R. Domingo, M. Arnó, J. Andrés, *J. Am. Chem. Soc.* **1998**, *120*, 1617–1618; h) V. Branchadell, *Int. J. Quantum Chem.* **1997**, *61*, 381–388.
[27] a) Y. Zhao, D. G. Truhlar, *Theor. Chem. Acc.* **2008**, *120*, 215–241; b) Y. Zhao, D. G. Truhlar, *Acc. Chem. Res.* **2008**, *41*, 1157–1167.
[28] a) T. H. Dunning Jr, *J. Chem. Phys.* **1989**, *90*, 1007–1023; b) D. E. Woon, T. H. Dunning Jr, *J. Chem. Phys.* **1993**, *98*, 1358–1371.
[29] M. J. Frisch, G. W. Trucks, H. B. Schlegel, G. E. Scuseria, M. A. Robb, J. R. Cheeseman, J. A. Montgomery Jr, T. Vreven, K. N. Kudin, J. C. Burant, J. M. Millam, S. S. Iyengar, J. Tomasi, V. Barone, B. Mennucci, M. Cossi, G. Scalmani, N. Rega, G. A. Petersson, H. Nakatsuji, M. Hada, M. Ehara, K. Toyota, R. Fukuda, J. Hasegawa, M. Ishida, T. Nakajima, Y. Honda, O. Kitao, H. Nakai, M. Klene, X. Li, J. E. Knox, H. P. Hratchian, J. B. Cross, C. Adamo, J. Jaramillo, R. Gomperts, R. E. Stratmann, O. Yazyev, A. J. Austin, R. Cammi, C. Pomelli, J. W. Ochterski, P. Y. Ayala, K. Morokuma, G. A. Voth, P. Salvador, J. J. Dannenberg, V. G. Zakrzewski, S. Dapprich, A. D. Daniels, M. C. Strain, O. Farkas, D. K. Malick, A. D. Rabuck, K. Raghavachari, J. B. Foresman, J. V. Ortiz, Q. Cui, A. G. Baboul, S. Clifford, J. Cioslowski, B. B. Stefanov, G. Liu, A. Liashenko, P. Piskorz, I. Komaromi, R. L. Martin, D. J. Fox, T. Keith, M. A. Al-Laham, C. Y. Peng, A. Nanayakkara, M. Challacombe, P. M. W. Gill, B. Johnson, W. Chen, M. W. Wong, C. Gonzalez, J. A. Pople, *Gaussian 03*, Revision B.04, Gaussian Inc., Pittsburgh, PA, **2003**.
[30] E. J. Bylaska, W. A. de Jong, N. Govind, K. Kowalski, T. P. Straatsma, M. Valiev, D. Wang, E. Apra, T. L. Windus, J. Hammond, P. Nichols, S. Hirata, M. T. Hackler, Y. Zhao, P. Fan, R. J. Harrison, M. Dupuis, D. M. A. Smith, J. Nieplocha, V. Tipparaju, M. Krishnan, Q. Wu, T. Van Voorhis, A. A. Auer, M. Nooijen, E. Brown, G. Cisneros, G. I. Fann, H. Fruchtl, J. Garza, K. Hirao, R. Kendall, J. A. Nichols, K. Tsemekhman, K. Wolinski, J. Anchell, D. Bernholdt, P. Borowski, T. Clark, D. Clerc, H. Dachsel, M. Deegan, K. Dyall, D. Elwood, E. Glendening, M. Gutowski, A. Hess, J. Jaffe, B. Johnson, J. Ju, R. Kobayashi, R. Kutteh, Z. Lin, R. Littlefield, X. Long, B. Meng, T. Nakajima, S. Niu, L. Pollack, M. Rosing, G. Sandrone, M. Stave, H. Taylor, G. Thomas, J. van Lenthe, A. Wong, Z. Zhang, *NWChem, A Computational Chemistry Package for Parallel Computers*, version 5.1.1, Pacific Northwest National Laboratory, Richland, Washington 99352-099, USA, **2007**.
[31] a) J. Sauer, *Angew. Chem. Int. Ed. Engl.* **1967**, *6*, 16–33; b) J. Sauer, R. Sustmann, *Angew. Chem. Int. Ed. Engl.* **1980**, *19*,

779–807; c) A. Z. Bradley, M. G. Kociolek, R. P. Johnson, *J. Org. Chem.* **2000**, *65*, 7134–7138.
[32] C. Gonzalez, H. B. Schlegel, *J. Phys. Chem.* **1990**, *94*, 5523–5527.
[33] a) A. Moyano, M. A. Pericas, E. Valenti, *J. Org. Chem.* **1989**, *54*, 573–582; b) I. Morao, B. Lecea, F. P. Cossío, *J. Org. Chem.* **1997**, *62*, 7033–7036; c) F. P. Cossío, I. Morao, H. Jiao, P.v. R. Schleyer, *J. Am. Chem. Soc.* **1999**, *121*, 6737–6746.
[34] J. Tomasi, M. Persico, *Chem. Rev.* **1994**, *94*, 2027–2033.
[35] a) A. Klamt, G. Schüürmann, *J. Chem. Soc. Perkin Trans. 2* **1993**, 799–805; b) A. Klamt, V. Jonas, T. Buerger, J. C. W. Lohrenz, *J. Phys. Chem. A* **1998**, *102*, 5074–5085.
[36] a) L. R. Domingo, *J. Org. Chem.* **2001**, *66*, 3211–3214; b) L. R. Domingo, M. T. Picher, J. Andrés, V. S. Safont, *J. Org. Chem.* **1997**, *62*, 1775–1778; c) L. R. Domingo, M. T. Picher, J. Andrés, V. Moliner, V. S. Safont, *Tetrahedron* **1996**, *52*, 10693–10704.
[37] a) C. J. Cramer, D. G. Truhlar, *Acc. Chem. Res.* **2008**, *41*, 760–768; b) A. V. Marenich, R. M. Olson, C. P. Kelly, C. J. Cramer, D. G. Truhlar, *J. Chem. Theory Comput.* **2007**, *3*, 2011–2033.
[38] a) M. W. Schmidt, K. K. Baldridge, J. A. Boatz, S. T. Elbert, M. S. Gordon, J. H. Jensen, S. Koseki, N. Matsunaga, K. A. Nguyen, S. Su, T. L. Windus, M. Dupuis, J. A. Montgomery, *J. Comput. Chem.* **1993**, *14*, 1347–1363; b) M. Higashi, A. V. Marenisch, R. M. Olson, A. C. Chamberlin, J. Pu, C. P. Kelly, J. D. Thompson, J. D. Xidos, J. Li, T. Zhu, G. D. Hawkins, Y. Y. Chuang, P. L. Fast, B. J. Lynch, D. A. Liotard, D. Rinaldi, J. Gao, C. J. Cramer, D. G. Thruhlar, *GAMESSPLUS*, University of Minnesota, Minneapolis, **2009**.
[39] a) A. E. Reed, F. Weinhold, *J. Chem. Phys.* **1985**, *83*, 1736–1740; b) A. E. Reed, L. A. Curtiss, F. Weinhold, *Chem. Rev.* **1988**, *88*, 899–926.
[40] E. D. Glendening, A. E. Reed, J. E. Carpenter, F. Weinhold, *NBO* Version 3.1, Madison, Wisconsin, **1988**.
[41] G. Schaftenaar, J. H. Noordik, *J. Comput.-Aided Mol. Des.* **2000**, *14*, 123–134.
[42] *Jmol*: an open-source Java viewer for chemical structures in 3D,http://www.jmol.org/.

Received: August 24, 2010
Published Online: December 9, 2010

